Majorana Fermions in Spin-Singlet Nodal Superconductors with Coexisting Noncollinear Magnetic Order

Yuan-Ming Lu[1,2] and Ziqiang Wang[3]

[1]*Department of Physics, University of California, Berkeley, California 94720, USA*
[2]*Materials Science Division, Lawrence Berkeley National Laboratories, Berkeley, California 94720, USA*
[3]*Department of Physics, Boston College, Chestnut Hill, Massachusetts 02467, USA*

Realizations of Majorana fermions in solid state materials have attracted great interest recently in connection to topological order and quantum information processing. We propose a novel way to create Majorana fermions in superconductors. We show that an incipient noncollinear magnetic order turns a spin-singlet superconductor with nodes into a topological superconductor with a stable Majorana bound state in the vortex core, at a topologically stable magnetic point defect, and on the edge. We argue that such an exotic non-Abelian phase can be realized in extended $t-J$ models on the triangular and square lattices. It is promising to search for Majorana fermions in correlated electron materials where nodal superconductivity and magnetism are two common caricatures.

A Majorana fermion is an electrically neutral fermion whose antiparticle is itself [1]. In recent years, Majorana fermions have attracted growing attention in condensed matter physics [2–4]. Specifically, Majorana fermions can be realized as zero-energy bound states in the vortex core or on the edge of certain two-dimensional super-conductors. Instead of the usual Bose or Fermi statistics, these vortices obey non-Abelian statistics [5–10] as a manifestation of topological order [11,12]. Due to this remarkable feature, Majorana bound states (MBSs) can be utilized for topologically protected qubits in fault-tolerant quantum computation [2,13,14]. Several systems have been proposed to realize MBSs, such as even-denominator fractional quantum Hall states [5,6,8,15], $p + ip$ superconductors [8–10] and superfluids [16,17], superconductor-topological insulator interfaces [18–21], s-wave Rashba superconductors [22–24] and spin-orbit-coupled nodal superconductors [25].

In this Letter, we present a novel realization of MBSs in spin-singlet superconductors with nodal excitations. We show that when a coexisting noncollinear magnetic order (NCMO) develops with a wave vector connecting two nodes at opposite momenta, there will be one MBS in each vortex core and on the edge of such topological superconductors. Moreover, each stable point defect of the NCMO also hosts a MBS. We demonstrate our proposal with two explicit examples. The first one is a nodal $d + id$ superconductor [26] coexisting with 1×3 (or 3×3) coplanar magnetic order on the triangular lattice. We argue that this state is likely to be realized in a doped t-J_2 model on the triangular lattice and is relevant for the sodium cobaltate superconductors $Na_xCoO_2 \cdot yH_2O$ near $x = 1/3$ [26,27]. The second example is a $d_{x^2-y^2}$ superconductor with coexisting $\mathbf{Q} = (Q_0, Q_0)$ NCMO on the square lattice which may be realized in a doped t-J_1-J_2-J_3 model on the

square lattice. Many strongly correlated materials, from high-T_c cuprates to heavy-fermion compounds, exhibit the d-wave superconductivity [28,29] in proximity to Ref. [30] or coexisting with [29,31] magnetic orders. Our findings suggest that Majorana fermions may exist in correlated electron materials with magnetic frustration and nodal superconductivity.

We begin with a general discussion. The low-energy excitations of a nodal superconductor are massless Dirac fermions with linear dispersion. Our basic idea is to create a topological superconductor by adding a proper mass to the nodal fermions. Consider the spin-singlet case with n pairs of isolated nodes located at crystal momenta $\pm \mathbf{q}_\ell$, $\ell = 1, \ldots, n$. Expanding around the nodes, the low-energy BCS Hamiltonian describing the quasiparticle excitations has a generic form in the Nambu basis $\Psi_{\ell \mathbf{k}} \equiv (c_{\mathbf{q}_\ell + \mathbf{k}, \uparrow}, c^\dagger_{-\mathbf{q}_\ell - \mathbf{k}, \downarrow}; c_{-\mathbf{q}_\ell + \mathbf{k}, \downarrow}, -c^\dagger_{\mathbf{q}_\ell - \mathbf{k}, \uparrow})^T$ for each pair of nodes at opposite momenta:

$$\mathcal{H}_{\text{eff}} = \sum_{\ell, \mathbf{k}} \Psi^\dagger_{\ell \mathbf{k}} H_{\ell \mathbf{k}} \Psi_{\ell \mathbf{k}}, \qquad H_{\ell \mathbf{k}} = (\mathbf{n}_{\ell \mathbf{k}} \cdot \vec{\tau}) \sigma_z, \quad (1)$$

and $\mathbf{n}_{\ell \mathbf{k}} = (\text{Re}\Delta_{\mathbf{q}_\ell + \mathbf{k}}, -\text{Im}\Delta_{\mathbf{q}_\ell + \mathbf{k}}, \xi_{\mathbf{q}_\ell + \mathbf{k}}) = \sum_\alpha k_\alpha \vec{v}^\ell_\alpha + \mathcal{O}(|\mathbf{k}|^2)$ with $\alpha = x, y$. Here $\Delta_{\mathbf{k}}$ is the pairing gap function and $\xi_{\mathbf{k}}$ the kinetic energy. $\vec{\tau}$ and $\vec{\sigma}$ are Pauli matrices operating in the particle-hole (Nambu) and spin sectors, respectively. A unitary rotation $U \equiv \exp[i \vec{\phi}_\ell \cdot \vec{\tau}]$ turns $H_{\ell \mathbf{k}}$ into $U^\dagger H_{\ell \mathbf{k}} U = (k_1 \tau_x + k_2 \tau_y) \sigma_z$ where $k_{1,2}$ are linearly independent combinations of k_x and k_y [32].

Let's focus on the ℓth pair of nodes at $\pm \mathbf{q}_l$. Clearly, a gap will be generated by adding a generic mass term of the form $\tau_0(\sigma_x \text{Re}M - \sigma_y \text{Im}M)$ to the Hamiltonian,

$$U^\dagger H'_{\ell \mathbf{k}} U = (k_1 \tau_x + k_2 \tau_y) \sigma_z + \tau_0(\sigma_x \text{Re}M - \sigma_y \text{Im}M),$$
$$(2)$$

where M is a complex order parameter. This is nothing but the effective Hamiltonian for proximity induced s-wave superconductivity on the surface of a 3D topological insulator [18], with M playing the role of the superconducting (SC) order parameter. The latter is known to contain a single MBS in the vortex core. In the present context of singlet nodal superconductors, the physical origin of the local order M turns out to be a *noncollinear* (coplanar) magnetic order described by

$$\mathcal{H}_{cp} = \sum_{\mathbf{r}}[M(S_{\mathbf{r}}^x + iS_{\mathbf{r}}^y)e^{i2\mathbf{q}_0 \cdot \mathbf{r}} + \text{H.c.}]$$

$$= \sum_{\ell\mathbf{k}} Mc_{\mathbf{q}_\ell+\mathbf{k}+\mathbf{q}_0,\uparrow}^\dagger c_{\mathbf{q}_\ell+\mathbf{k}-\mathbf{q}_0,\downarrow} + \text{H.c.}, \quad (3)$$

where $S_{\mathbf{r}}^a = \sum_{\alpha\beta} c_{\mathbf{r}\alpha}^\dagger \sigma_{\alpha\beta}^a c_{\mathbf{r}\beta}/2$, $a = x$, y, z are the spin operators at site $\mathbf{r}$. When the ordering wave vector $2\mathbf{q}_0$ connects the nodes at $\pm\mathbf{q}_\ell$, the magnetic scattering generates precisely the mass term in Eq. (2). Since $SO(3)$ spin-rotational symmetry is completely broken, such a NCMO bears a topologically stable point defect [33] characterized by the nontrivial homotopy $\pi_1(SO(3)) = \mathbb{Z}_2$. The SC vortex in the Fu-Kane model [18] maps exactly to such a stable point defect of NCMO M in (2). Therefore, there is a non-Abelian MBS in each stable point defect of noncollinear magnetic order.

Remarkably, the NCMO gives rise to a non-Abelian topological superconductor since, among the two (even and odd) combinations $c_{\mathbf{k},e(o)} \equiv \frac{1}{\sqrt{2}}(c_{\mathbf{q}_\ell+\mathbf{k},\uparrow} \pm c_{-\mathbf{q}_\ell+\mathbf{k},\downarrow})$, the odd combination is driven into the topologically nontrivial weak-pairing phase [8] by the mass gap, while the even one to the trivial strong-pairing phase. The situation is analogous to a doubled-layer $\nu = 1/2$ fractional quantum Hall system, where the Abelian (331) state can be driven to a non-Abelian Pfaffian state by interlayer tunneling [8,34,35]. The existence of a single MBS in the SC vortex core is thus implied by the vortex-boundary correspondence [8]. Note that the existence of a single MBS will not be affected by the other nodal fermions [25]. They are spin-flip scattered either to finite energy away from the Fermi level or, in special cases, to different nodes not connected by pairing; they either remain gapless or are gapped out in the magnetic sector.

We stress that it is crucial to require the magnetic order to be *noncollinear*: a collinear spin order, such as $\mathcal{H}_{cl} = 2m\sum_{\mathbf{r}} S_{\mathbf{r}}^x \cos(2\mathbf{q}_0 \cdot \mathbf{r}) = \sum_{\ell\mathbf{k}}\sum_\sigma mc_{\mathbf{q}_\ell+\mathbf{k}+\mathbf{q}_0,\sigma}^\dagger c_{\mathbf{q}_\ell+\mathbf{k}-\mathbf{q}_0,\bar\sigma} +$ H.c., not only drives the Nambu pair $(c_{\mathbf{q}_0+\mathbf{k},\uparrow}, c_{-\mathbf{q}_0-\mathbf{k},\downarrow}^\dagger)$, but also $(c_{-\mathbf{q}_0+\mathbf{k},\uparrow}, c_{\mathbf{q}_0-\mathbf{k},\downarrow}^\dagger)$ into the weak-pairing phase, creating two copies of weak-pairing $p + ip$ superconductors with two MBSs in the vortex core and two counterpropagating Majorana modes on the edge. Thus, there will be no stable MBSs in this case since the two branches can scatter and open up a gap in the energy spectrum.

On general grounds, NCMO can be realized in frustrated systems from the residual spin-spin interactions between the nodal fermions in the SC state. Its presence (3) breaks both inversion and spin rotational symmetry. Thus, the spin-singlet pairing can mix with triplet pairing. When the triplet pairing amplitude is small compared to $|M|$, the system will stay in the gapped non-Abelian topological phase. In the opposite limit, a dominant one-component chiral triplet pairing state is well known to be in the non-Abelian weak-pairing phase [8,9]. Therefore we expect the non-Abelian topological superconductor to be stable against the mixing between singlet and triplet pairing. We next demonstrate the above predictions with direct calculations in two specific examples on the triangular and the square lattices.

We start with the nodal chiral superconductors on the triangular lattice proposed for the SC state of hydrated sodium cobaltates [36]. Recent NMR measurements find strong evidence for singlet pairing [27,37,38] with nodal excitations at a critical doping $x_c \approx 0.26$ [38]. Specifically, it was shown [26] that second nearest neighbor (NN) $d + id$ pairing can be the dominant pairing channel on the electron doped triangular lattice where the complex gap function has six isolated zeros inside the first Brillouin zone (BZ). The Fermi surface (FS) crosses these nodes at a critical doping x_c, producing six Dirac points as shown in Fig. 1(a). The SC states at $x < x_c$ and $x > x_c$ are separable by a topological phase transition. We thus consider a simple effective pairing Hamiltonian

$$\mathcal{H} = \sum_{\mathbf{k}\sigma} \xi_{\mathbf{k}} c_{\mathbf{k}\sigma}^\dagger c_{\mathbf{k}\sigma} + \sum_{\mathbf{k}}(\Delta_{\mathbf{k}} c_{\mathbf{k}\uparrow} c_{-\mathbf{k}\downarrow} + \text{H.c.}), \quad (4)$$

where $\xi_{\mathbf{k}}$ is the band dispersion with hopping amplitudes $(t_1, t_2, t_3) = (-202, 35, 29)$ meV for the first three NN [26]. $\Delta_{\mathbf{k}} = 2\Delta_2[\cos(k_1 - k_2) + e^{i2\pi/3}\cos(2k_1 + k_2) + e^{i4\pi/3}\cos(k_1 + 2k_2)]$ is the second NN $d + id$ pairing gap function in the basis $\mathbf{k} = k_1\vec{b}_1 + k_2\vec{b}_2$ shown in Fig. 1(a). The six Dirac nodes (N_i, $i = 1, \ldots, 6$) are located at $(k_1, k_2) = \pm(2\pi/3, 0)$, $\pm(0, 2\pi/3)$, and $\pm(2\pi/3, -2\pi/3)$.
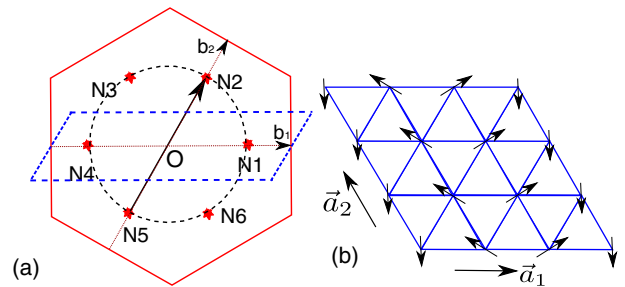

FIG. 1 (color online). (a) The first BZ of the triangular lattice and the six nodes (N_i) of the second NN $d + id$ pairing gap function. The normal state FS (dashed circle) crosses the gap nodes at doping x_c for the nodal chiral superconductor. The arrow indicates the wave vector of the 1×3 NCMO shown in (b) with the magnetic zone shown by the dashed parallelogram. $\vec{a}_{1,2}$ are two primitive lattice vectors. The reciprocal vectors are $\vec{b}_{1,2}$ with $\vec{a}_i \cdot \vec{b}_j = \delta_{i,j}$.

Such a $d + id$ superconductor exhibits quantized spin Hall conductance [8] associated with the winding number W of the unit vector $\hat{n}_{\mathbf{k}} = (\mathrm{Re}\Delta_{\mathbf{k}}, -\mathrm{Im}\Delta_{\mathbf{k}}, \xi_{\mathbf{k}})/E_{\mathbf{k}}$ where $E_{\mathbf{k}} = \sqrt{\xi_{\mathbf{k}}^2 + |\Delta_{\mathbf{k}}|^2}$. When the FS lies inside the Dirac points $(x > x_c)$, $W = -2$ and there are two counterclockwise-propagating chiral fermions on the edge; each is charge neutral but carries spin $\hbar/2$ [26]. When the FS encloses the six gap nodes $(x < x_c)$, $W = 4$ and there are four spin-carrying chiral fermions on the edge.

A NCMO described by $\mathcal{H}_{\mathrm{cp}}$ in Eq. (3), with $2\mathbf{q}_0$ pointing from N_{i+3} to N_i [Fig. 1(a)], produces a mass gap for the nodal fermions as discussed above. The magnetic order corresponds to the 1×3 coplanar pattern shown in Fig. 1(b). The nodal chiral superconductor is thus turned into a non-Abelian topological superconductor with a winding number $W = +1$. Similar to a spinless $p + ip$ superconductor [8], it supports a single MBS in the vortex core and on the sample edge. To demonstrate the latter, we calculate explicitly the edge spectrum of $\mathcal{H} + \mathcal{H}_{\mathrm{cp}}$ on a cylinder with two parallel edges along the $\vec{a}_2$ direction. The solutions of the BdG equations [39] are shown in Fig. 2(a) for $\Delta_2 = 150$ meV and $M = 200$ meV. The bulk excitations are completely gapped since the scattering wave vector $2\mathbf{q}_0$ not only connects the Nambu pair (N_5, N_2) but also (N_3, N_4) and (N_1, N_6) in the magnetic sector. There is a single branch of the gapless Majorana mode crossing $k = 0$ that is localized at the edges. We also performed direct calculations of the SC vortex and the magnetic defect spectrum on 90×30 periodic lattices in the presence of a vortex-antivortex pair and a pair of stable point defects, respectively [39]. The results are shown in Figs. 2(b) and 2(c). Clearly, a single zero-energy MBS emerges with a density profile localized in the SC vortex core and at the magnetic defect. Note that since the topological superconductor is in the gapped phase, its stability is protected against perturbations that are not strong enough to destroy the gap and create a quantum phase transition into a different state. As a result, the non-Abelian topological phase supporting MBS proposed here is not limited to very particular parameters and will remain stable when, e.g., small variations in doping around x_c cause the FS to deviate from the gap nodes, or a small NN pairing component induced by a subdominant NN exchange J_1 causes the gap nodes to shift and the magnetic ordering wave vector to not precisely connect the pair of nodes at opposite momenta.

To see how the 1×3 NCMO can arise microscopically, we consider the second NN antiferromagnetic Heisenberg model, i.e., the J_2 model, on the triangular lattice. The classical ground state is well known to have 3×3 NCMO [40,41]: on each of the three sublattices connected by second-NN bonds the spins exhibit 120 degree coplanar order. There is a large ground state degeneracy due to the relative spin orientations. This 3×3 NCMO already
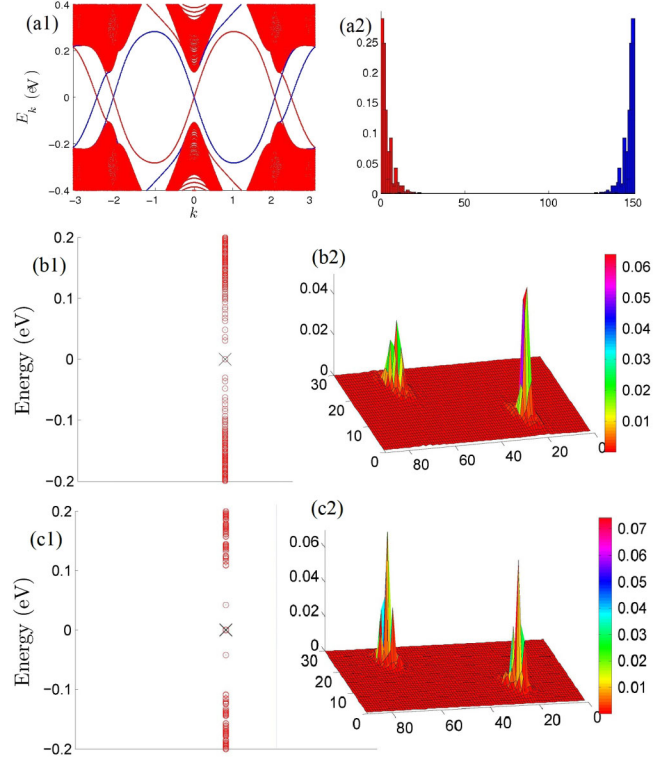

FIG. 2 (color online). Edge state spectrum (a1) obtained on a cylinder of length $L_1 = 150$. Vortex spectrum (b1) and magnetic defect spectrum (c1) obtained on 90×30 triangular lattices with periodic boundary conditions. The momentum k of the Majorana mode in (a1) is along $\vec{b}_2$ direction in the magnetic zone in Fig. 1. Right column: The density profiles of the zero-energy MBS. The SC vortex-antivortex pair (b2) and the pair of magnetic defects (c2) are placed at $(r_1, r_2) = (23.5, 8.5)$ and $(68.5, 23.5)$, where $\mathbf{r} = r_1\vec{a}_1 + r_2\vec{a}_2$.

induces a single MBS crossing $k = 0$ in the edge spectrum [39]. Quantum fluctuations would lift the degeneracy through the order-due-to-disorder mechanism [42–44], and the true quantum ground state has the 1×3 order. We have carried out a Schwinger-boson large-S expansion study [39] of the spin-S Heisenberg J_2 model and found that when S is larger than a critical value $S_c \approx 0.17$ (such as for spin-1/2), the system develops the 1×3 NCMO shown in Fig. 1(b). This suggests that if the residual interactions between the nodal fermions are dominated by the second NN Heisenberg exchange J_2, the 1×3 NCMO is likely to develop with $2\mathbf{q}_0$ connecting the gap nodes at opposite momenta as shown in Fig. 1. More intriguingly, to the extent that J_2 would favor a second NN $d + id$ resonance valence bond pairing state, it is likely that both the nodal chiral superconductor and the NCMO can emerge from the same exchange interaction in a doped t-J_2 model.

We turn to the second example of a more familiar nodal $d_{x^2-y^2}$ superconductor on the square lattice described by the same pairing Hamiltonian $\mathcal{H}$ in Eq. (4), but with the
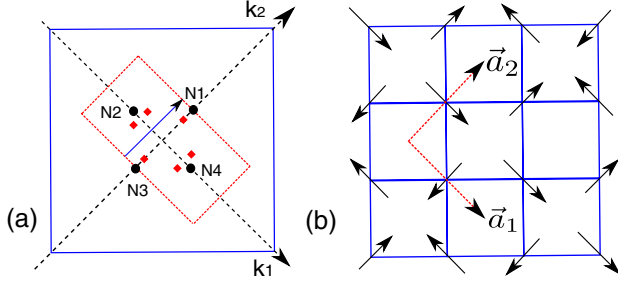
FIG. 3 (color online). (a) The first BZ of the square lattice. Black circles denote the four nodes (N_i) where the FS intersects the nodal lines of the $d_{x^2-y^2}$ pairing gap function. The NCMO with $\mathbf{Q}_0 = (\pi/2, \pi/2)$ (black arrow) turns them into six red diamonds inside the magnetic zone (red rectangle). (b) The spin configuration of the $(\pi/2, \pi/2)$ NCMO.

dispersion $\xi_{\mathbf{k}} = -2t[\cos(k_1 + k_2) + \cos(k_1 - k_2)] - \mu$ for NN hopping t, and the NN $d_{x^2-y^2}$ pairing gap function $\Delta_{\mathbf{k}} = 2\Delta_1[\cos(k_1 + k_2) - \cos(k_1 - k_2)]$. The momentum is defined as $\mathbf{k} = k_1\vec{b}_1 + k_2\vec{k}_2$ as shown in Fig. 3. The four nodal points are located at $N_{1,3}:(k_1 = 0, k_2 = \pm q_0)$ and $N_{2,4}:(k_1 = \pm q_0, k_2 = 0)$ with $q_0 = \arccos(-\frac{\mu}{4t})$. A NCMO described by $\mathcal{H}_{\mathrm{cp}}$ in Eq. (3) with ordering momentum $\mathbf{Q}_0 = (Q_0, Q_0) = 2\mathbf{q}_0 = 2q_0\vec{b}_2$ gaps out the $(c_{N_3,\uparrow}, c^\dagger_{N_1,\downarrow})$ branch and creates a single MBS. Figure 3 shows a specific example with $\mu = -2\sqrt{2}t$ and $q_0 = \pi/4$, together with the spin configuration. In this case, the commensurate magnetic order cannot gap out all nodes since the Hamiltonian is still invariant under time reversal followed by a lattice translation [45]. As shown in Fig. 3(a), the NCMO turns the original four spin-degenerate nodes (black circles) into six non-degenerate ones (red diamonds). The vanished pair of nodes is gapped out by the magnetic mass (3) and enters the weak-pairing phase. The calculated edge spectra along (1,1) direction is plotted in Fig. 4 near the magnetic zone boundary, showing the zero energy MBS localized on the parallel edges. Similar results are obtained at other commensurate values of q_0 such as $q_0 = \pi/3$. Since the gapless bulk excitations are located at different momenta, the MBS near $k_2 = \pi$ is expected to be stable against impurities and the mixing with bulk excitations [25]. For a generic doping, q_0 is incommensurate with the lattice and a corresponding incommensurate NCMO could produce a full gap for bulk excitations.

A remarkable feature seen in Fig. 4 is that the Majorana mode on the edge is dispersionless; i.e., it is localized and does not possess a chirality. This boundary zero-energy flat band, which begins and terminates at the reconstructed nodes of bulk excitations, is a direct consequence of the nontrivial $\mathbb{Z}_2$ winding number (topological index of class D in $d = 1$ [46]) of the momentum-space Hamiltonian around the nodes [47] in Fig. 3(a). The Majorana flat band is analogous to the Fermi arc on the 2D surface of
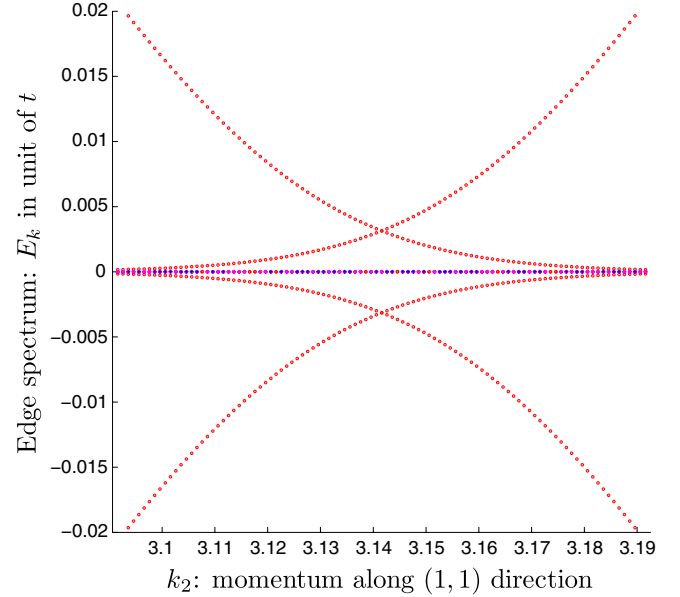

FIG. 4 (color online). Edge spectra as a function of momentum k_2 near the magnetic zone boundary for the $d_{x^2-y^2}$ superconductor with $(\pi/2, \pi/2)$NCMO. The spectrum is zoomed in around $k_2 = \pi$ where a flat band of zero energy MBS is localized on the two edges (blue and magenta). Red dispersing lines are the bulk states with nodes located at $k_2 \approx \pi \pm 0.04$.

3D time-reversal symmetry breaking Weyl semimetals proposed for pyrochlore iridates [48]. Nevertheless, the time reversal symmetry breaking by the magnetic order (3) can induce a small imaginary part in Δ_1, which would generate a full gap for bulk excitation and a single MBS on the edge dispersing across $k_2 = \pi$ with a well-defined chirality [39].

It is possible to realize such a NCMO in the Heisenberg J_1-J_2-J_3 model on the square lattice. The classical ground state has NCMO with momenta $\mathbf{Q}_0 = Q_0\vec{b}_{1,2}$ where $\cos(Q_0) = -J_1/(2J_2 + 4J_3)$ for $4J_3 + 2J_2 \geq J_1$ and $J_3 \geq J_2/2$ [49,50]. There is numerical evidence that the latter survives in the quantum $S = 1/2$ Heisenberg J_1-J_2-J_3 model in a wide parameter range [51,52]. We thus expect that such non-Abelian magnetic d-wave superconductors may be realized in certain parameter regime of the doped t-J_1-J_2-J_3 model.

In summary, we proposed a new type of non-Abelian topological superconductors. They emerge when spin-singlet superconductors with isolated nodes coexist with NCMO at the wave vector connecting the nodes at opposite momenta. Majorana fermions arise in the vortex core and on the edge of such magnetic superconductors. Remarkably, each stable point defect of the noncollinear magnetic order also hosts a single MBS. Since magnetism and unconventional superconductivity are common features of strong correlation, our findings suggest searching for the MBS in correlated materials with magnetic frustration and nodal superconductivity.

[1] F. Wilczek, Nat. Phys. **5,** 614 (2009).
[2] C. Nayak, S. H. Simon, A. Stern, M. Freedman, and S. Das Sarma, Rev. Mod. Phys. **80,** 1083 (2008).
[3] M. Z. Hasan and C. L. Kane, Rev. Mod. Phys. **82,** 3045 (2010).
[4] X.-L. Qi and S.-C. Zhang, Rev. Mod. Phys. **83,** 1057 (2011).
[5] G. Moore and N. Read, Nucl. Phys. **B360,** 362 (1991).
[6] C. Nayak and F. Wilczek, Nucl. Phys. **B479,** 529 (1996).
[7] E. Fradkin, C. Nayak, A. Tsvelik, and F. Wilczek, Nucl. Phys. **B516,** 704 (1998).
[8] N. Read and D. Green, Phys. Rev. B **61,** 10 267 (2000).
[9] D. A. Ivanov, Phys. Rev. Lett. **86,** 268 (2001).
[10] M. Stone and S.-B. Chung, Phys. Rev. B **73,** 014505 (2006).
[11] X. G. Wen and Q. Niu, Phys. Rev. B **41,** 9377 (1990).
[12] X. G. Wen, Phys. Rev. Lett. **66,** 802 (1991).
[13] A. Y. Kitaev, Ann. Phys. (Amsterdam) **303,** 2 (2003).
[14] S. Das Sarma, M. Freedman, and C. Nayak, Phys. Rev. Lett. **94,** 166802 (2005).
[15] Y.-M. Lu, Y. Yu, and Z. Wang, Phys. Rev. Lett. **105,** 216801 (2010).
[16] V. Gurarie, L. Radzihovsky, and A. V. Andreev, Phys. Rev. Lett. **94,** 230403 (2005).
[17] N. R. Cooper and G. V. Shlyapnikov, Phys. Rev. Lett. **103,** 155302 (2009).
[18] L. Fu and C. L. Kane, Phys. Rev. Lett. **100,** 096407 (2008).
[19] T. D. Stanescu, J. D. Sau, R. M. Lutchyn, and S. Das Sarma, Phys. Rev. B **81,** 241310 (2010).
[20] J. Linder, Y. Tanaka, T. Yokoyama, A. Sudbo, and N. Nagaosa, Phys. Rev. Lett. **104,** 067001 (2010).
[21] H. Weng, G. Xu, H. Zhang, S.-C. Zhang, X. Dai, and Z. Fang, Phys. Rev. B **84,** 060408 (2011).
[22] M. Sato, Y. Takahashi, and S. Fujimoto, Phys. Rev. Lett. **103,** 020401 (2009).
[23] J. D. Sau, R. M. Lutchyn, S. Tewari, and S. Das Sarma, Phys. Rev. Lett. **104,** 040502 (2010).
[24] J. Alicea, Phys. Rev. B **81,** 125318 (2010).
[25] M. Sato and S. Fujimoto, Phys. Rev. Lett. **105,** 217001 (2010).
[26] S. Zhou and Z. Wang, Phys. Rev. Lett. **100,** 217002 (2008).

[27] G.-q. Zheng, K. Matano, R. L. Meng, J. Cmaidalka, and C. W. Chu, J. Phys. Condens. Matter **18,** L63 (2006).
[28] C. C. Tsuei and J. R. Kirtley, Rev. Mod. Phys. **72,** 969 (2000).
[29] C. Pfleiderer, Rev. Mod. Phys. **81,** 1551 (2009).
[30] P. A. Lee, N. Nagaosa, and X.-G. Wen, Rev. Mod. Phys. **78,** 17 (2006).
[31] M. Sigrist and K. Ueda, Rev. Mod. Phys. **63,** 239 (1991).
[32] This is true as long as $\vec{v}_x^{\ell} \times \vec{v}_y^{\ell} \neq 0$, which is always satisfied by a nodal Dirac point. (k_1, k_2) can be viewed as the two-dimensional momenta in another coordinate system.
[33] H. Kawamura and S. Miyashita, J. Phys. Soc. Jpn. **53,** 4138 (1984).
[34] T.-L. Ho, Phys. Rev. Lett. **75,** 1186 (1995).
[35] N. Read and E. Rezayi, Phys. Rev. B **54,** 16 864 (1996).
[36] K. Takada, H. Sakurai, E. Takayama-Muromachi, F. Izumi, R. A. Dilanian, and T. Sasaki, Nature (London) **422,** 53 (2003).
[37] T. Fujimoto, G.-q. Zheng, Y. Kitaoka, R. L. Meng, J. Cmaidalka, and C. W. Chu, Phys. Rev. Lett. **92,** 047004 (2004).
[38] G.-q. Zheng, K. Matano, D. P. Chen, and C. T. Lin, Phys. Rev. B **73,** 180503 (2006).
[39] See Supplemental Material at http://link.aps.org/supplemental/10.1103/PhysRevLett.110.096403 for additional discussions.
[40] S. Katsura, T. Ide, and T. Morita, J. Stat. Phys. **42,** 381 (1986).
[41] T. Jolicoeur, E. Dagotto, E. Gagliano, and S. Bacci, Phys. Rev. B **42,** 4800 (1990).
[42] J. Villain, R. Bidaux, J.-P. Carton, and R. Conte, J. Phys. (Les Ulis, Fr.) **41,** 1263 (1980).
[43] C. L. Henley, Phys. Rev. Lett. **62,** 2056 (1989).
[44] A. V. Chubukov and T. Jolicoeur, Phys. Rev. B **46,** 11 137 (1992).
[45] E. Berg, C.-C. Chen, and S. A. Kivelson, Phys. Rev. Lett. **100,** 027003 (2008).
[46] A. P. Schnyder, S. Ryu, A. Furusaki, and A. W. W. Ludwig, Phys. Rev. B **78,** 195125 (2008).
[47] F. Wang and D.-H. Lee, Phys. Rev. B **86,** 094512 (2012).
[48] X. Wan, A. M. Turner, A. Vishwanath, and S. Y. Savrasov, Phys. Rev. B **83,** 205101 (2011).
[49] E. Rastelli, L. Reatto, and A. Tassi, J. Phys. C **19,** 6623 (1986).
[50] J. Ferrer, Phys. Rev. B **47,** 8769 (1993).
[51] P. Sindzingre, L. Seabra, N. Shannon, and T. Momoi, J. Phys. Conf. Ser. **145,** 012048 (2009).
[52] P. Sindzingre, N. Shannon, and T. Momoi, J. Phys. Conf. Ser. **200,** 022058 (2010).